Proceedings of 14th IOE Graduate Conference
Peer Reviewed
Year: 2023 Month: December Volume: 14
ISSN: 2350-8914 (Online), 2350-8906 (Print)

Prediction of Rock Mass Quality and Stability Assessment of the Headrace Tunnel of Marsyangdi PRoR Hydropower Project

Garima Shrestha [a], Krishna Kanta Panthi [b], Ghan Bahadur Shrestha [c], Nabaraj Neupane [d]

[a, c, d] *Department of Civil Engineering, Pashchimanchal Campus, IOE, Tribhuvan University, Nepal*
[b] *Department of Geoscience and Petroleum, NTNU, Norway*
[a] sthgarima@gmail.com

Abstract
In the construction of underground structures, the preconstruction stage investigation governs the output of the project. The properties of rock mass makes it inevitable that there will be some variation between actual and predicted rock mass condition, however the investigation helps reduce any unwanted results. It has been challenging to accurately predict rock mass quality and evaluate stress-induced problems in the Nepal Himalayas, where tunnel squeezing is a frequent occurrence in weak rock and in weakness zones. When tangential stress exceeds the strength of the rock mass, incompetent rock with high or moderate rock stress caused by moderate to high overburden may have tunnel squeezing issues. Surface geological mapping was done and stability analysis and support determination was carried out with use of different methods for the headrace tunnel of Marsyangdi PRoR Hydropower Project. An assessment was carried out to find out most favorable tunnel alignment with the help of geological map and discontinuity mapping done in course of the study. This paper presents longitudinal profile along the tunnel alignment, rock mass quality along the tunnel alignmnent and stability assessment results of three selected tunnel sections using semi-analytical, analytical and numerical methods.

Keywords
Rock mass quality, Stability assessment, Support Determination

1. Introduction

Nepal has a huge potential for hydroelectric power generation. The technical potential of Nepal is estimated to be 83 gigawatts (GW) among which 42 GW is considered to be economically viable [1]. Due to the topography and geology of Nepal underground structures are more favorable in many areas of Nepal. For the construction of every underground structure proper and well planned engineering geological investigations should be carried out. Rock mass being a complex material it is inevitable that there will be some variation between actual and predicted rock mass conditions, however they must be within acceptable range so that cost and time overrun are not excessive [2]. In hilly region, there will be high overburden pressure which will have direct impact in the stability of tunnels associated to squeezing, rock bursting and rock spalling. In the Nepal Himalayas, tunnel squeezing a common occurrence in weak rocks and in the weakness zones which are not able to bear significant stress [3]. The condition of rock mass quality is one of the key components for the economic optimality of any tunneling project and long-term stability. Therefore, proper engineering geological investigation is important for a reliable assessment of stability and overall cost of the project.

2. Brief on the Project

2.1 Project Description and Geology of the Area

The Marsyangdi PRoR Hydropower Project is located in Tanahun, Gorkha and Lamjung district in Gandaki Province of Nepal. The proposed headrace tunnel alignment of the project lies at 170 km west from Kathmandu. The tunnel alignment passes through hills having gentle rock slopes with topography variation from 400 masl to 877 masl. Geologically, the project area lies in lesser Himalayan region. Phyllite was the dominant rock found in the project area which ranged from pellitic phyllite to gritty phyllite whereas metasandstone and schist was found occasionally. Weathered terrain of phyllite were also observed at some places. Therefore, the tunnel alignment will mostly pass through phyllite rocks. A comprehensive field engineering geological field mapping was carried out covering the project area. Figure 2 shows the locations traversed during engineering geological field mapping. With the data collected, geological map of the project area was prepared and possible tunnel alignments were fixed with the use of output obtained from discontinuity

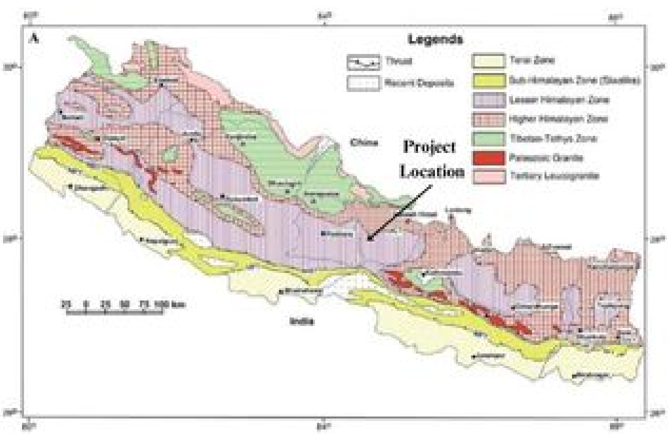

Figure 1: Geological Map of Nepal showing project location

mapping (Figure 3). As indicated in the figure the project area lies in Kuncha formation of Nuwakot group where phyllite rock mass found to be green to grey in color, fine to medium grained, thin to moderately foliated, slightly to moderately weathered, weak to medium strong which is in frequent intercalation with grey medium to coarse grained, thin to medium foliated, slight to moderately weathered, medium to strong metasandstone. There are also a few successions of quartzite bands. Pelitic phyllite is undulated, foliation planes seem planar in outcrop section but regionally undulated, locally folded. Quartz veins are present occasionally.

Figure 2 shows the locations traversed during the field work for surface mapping. With the data collected the geological map of the project area is prepared and suitable tunnel alignment fixed with use of output obtained from discontinuity mapping.

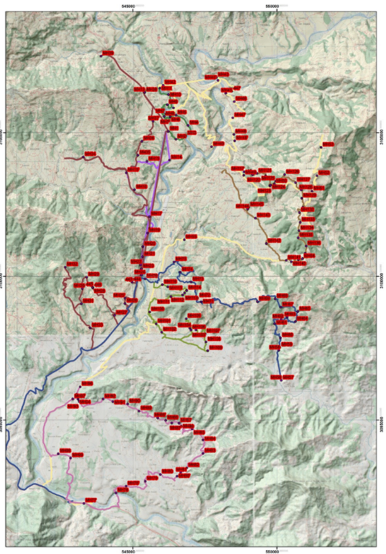

Figure 2: Locations traversed during the field work

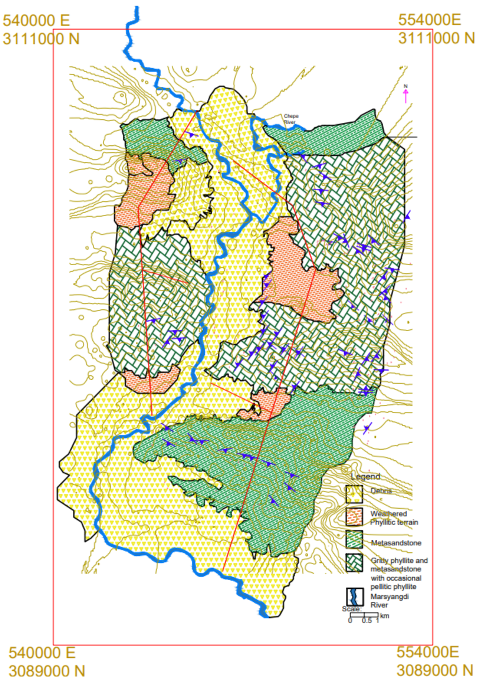

Figure 3: Geological Map of study area with Tunnel Alignment

2.2 Rock Mass Quality

Rock mass classification based on the Q-system was carried out along the headrace tunnel alignment. The Table 1 shows the different quality class according to the Q-value range given in [3]. The Figure 4 indicates the rock mass quality distribution along the tunnel alignment.

Table 1: Rock mass classification according to Q-system (Panthi, 2006)

		Q-values	
Rock Class	**Quality**	**Minimum**	**Maximum**
Class 1	Very good to excellent	100	1000
Class 2	Good	10	100
Class 3	Fair to Good	4	10
Class 4	Poor	1	4
Class 5	Very Poor	0.1	1
Class 6	Extremely Poor	0.01	0.1
Class 7	Exceptionally Poor	0.001	0.01

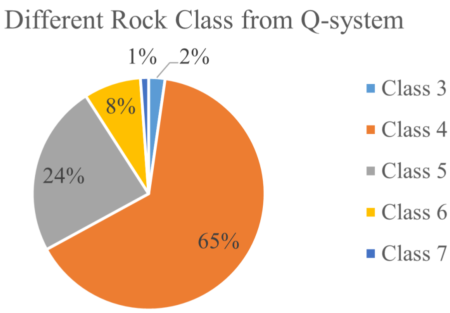

Figure 4: Different Rock Class from Q-system

Table 2 shows distribution of various types of rocks found along the tunnel alignment. With the use of existing geological maps and detailed geological mapping carried out engineering geological longitudinal section of the headrace tunnel was prepared (Figure 5 and Figure 6).

Table 2: Different rock types encounterd at different chainage of right tunnel alignment

Chainage	Rock Type	Q Value	Rock Mass Class
1+000	Gritty phyllite with occasional pelitic phyllite and metasandstone	1.67	Poor
2+000	Weathered Phyllite	0.22	Very Poor
3+670	Gritty phyllite and metasandstone with occasional pellitic phyllite	0.56	Very Poor
4+670	Weathered Phyllite	0.42	Very Poor
5+670	Gritty phyllite and metasandstone with occasional pellitic phyllite	1.25	Poor
6+670	Gritty phyllite and metasandstone with occasional pellitic phyllite	1.6	Poor
7+670	Gritty phyllite and metasandstone with occasional pellitic phyllite	2.08	Poor
8+670	Gritty phyllite and metasandstone with occasional pellitic phyllite	5.83	Fair
9+670	Gritty phyllite and metasandstone with occasional pellitic phyllite	0.08	Extremely Poor
10+485	Weathered Phyllite	0.6	Very Poor

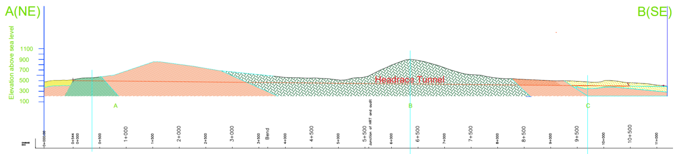

Figure 5: Longitduinal Profile along the right alignment

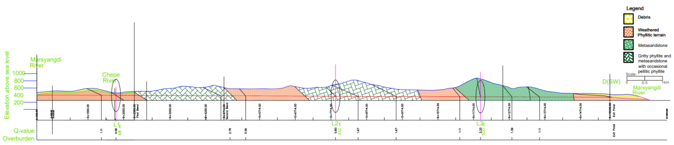

Figure 6: Longitudinal Profile along the left alignment

The rock mass class classification was carried out along the traversed area as indicated in FIgure 2. From inlet portal to chainage 1+000 poor rock class was found. Similarly the rock mass class from chainage 2+000 to 4+670 consists of very poor rock mass class. From chainage 5+670 to 7+670, the rock mass class is poor and from 7+670 to 8+670 is fair rock mass class type. Similarly, extremely poor quality rock mass was found from 8+670 up to chainage 9+670 and remaining downstream part of the tunnel alignment is mainly buried within the colluvial and alluvial deposit where it is expected that the rock mass of poor quality and colluvium and alluvium deposit persists.

Table 3: Different rock types encountered at different chainage of left tunnel alignmnet

Chainage	Rock Type	Q Value	Rock Mass Class
2+300	Weathered Phyllite	1.11	Poor
4+714	Gritty phyllite and metasandstone with occasional pellitic phyllite	1.81	Poor
6+029	Weathered Phyllite	2.21	Poor
8+8825	Gritty phyllite and metasandstone with occasional pellitic phyllite	1.78	Poor
10+095	Weathered Phyllite	0.83	Very Poor
13+415	Gritty phyllite with occasional pellitic phyllite and metasandstone	1.83	Poor
15+539	Weathered Phyllite	0.83	Very Poor

2.3 Discontinuity mapping

The rosette diagrams were prepared to assess the tunnel alignment (Figures 7, 8, 9, 10, and 11). As seen in the figure the favourability of the tunnel alignment varies greatly since the joints have orientation in many direction. With the help of this rosette diagram and the geological map, the most favorable tunnel alignment was selected (TAN). From figure 7 and 8 the tunnel alignment for right alignment at north of bend is at around 30° north. The rosette for south of bend is shown in the figure 8. The optimum tunnel alignment(TA1), which is north 355° east. Owing to the tunnel alignment selected for north of bend, the alternative alignment is not viable option for south of bend. So, the best fit alignment is chosen. The tunnel alignment selected is shown by TAS which is north 351° east.

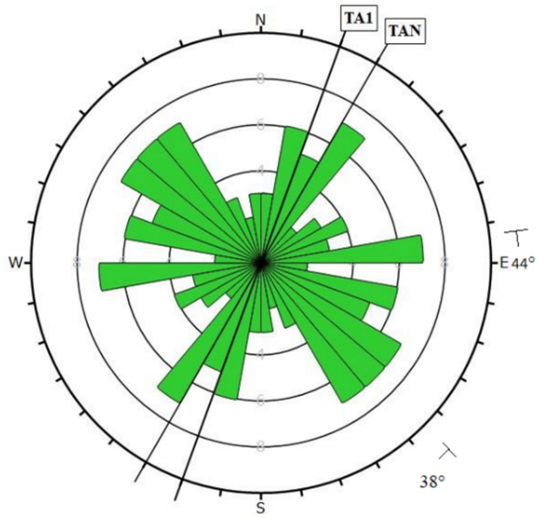

Figure 7: Rosette Diagram for North of bend for right alignment

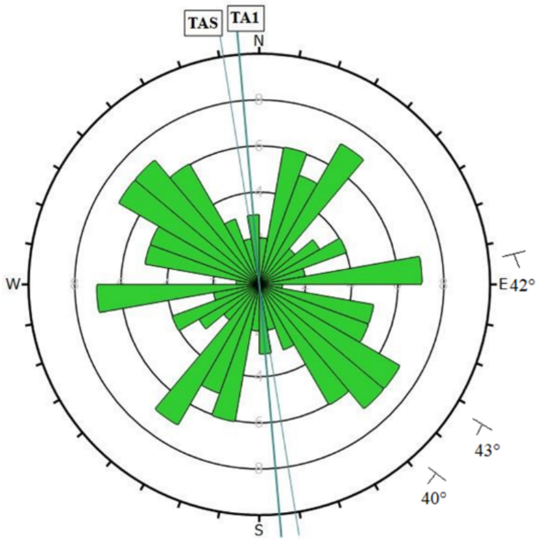

Figure 8: Rosette diagram for south of bend for right alignment

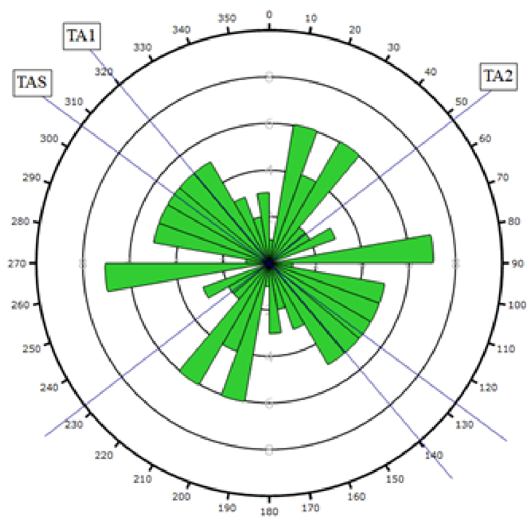

Figure 9: Rosette Diagram for North of 1st Bend for left alignment

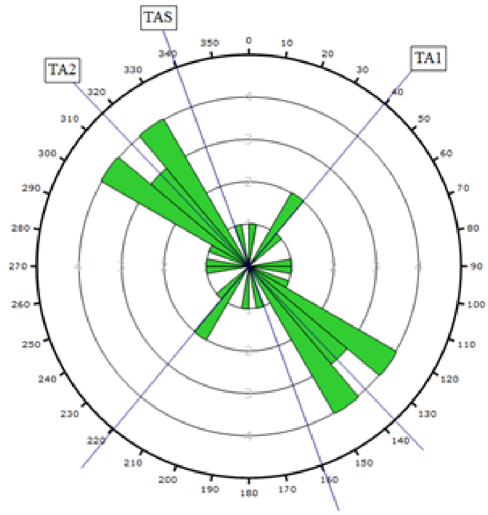

Figure 10: Rosette Diagram for tunnel between bend for left alignment

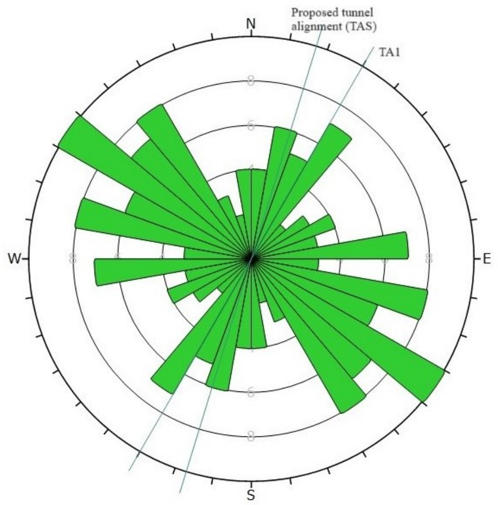

Figure 11: Rosette Diagram for South of Bend for left alignment

The above-mentioned rosette diagram figure 9, 10 and 11 shows most favorable tunnel alignment. With the help of this rosette diagram and the geological map, the most favorable tunnel alignment was selected (TAN). The rosette diagram shows most favorable tunnel alignment (TA1) at north 320° east. With the help of this rosette diagram and the geological map, the most favorable tunnel alignment was selected (TAN). The tunnel alignment at north of bend is at around north 305° east for north of bend of the left alignment.

The rosette diagram shows most favorable tunnel alignment (TA 1) at N40°E and N318°E. With the help of this rosette diagram and the geological map, the most favorable tunnel alignment was selected (TAN). The tunnel alignment at north of bend is at around N340°E for section between two bends of the left alignment The rosette diagram shows most favorable tunnel alignment (TA 1) at N30°E. With the help of this rosette diagram and the geological map, the most favorable tunnel alignment was selected (TAN). The tunnel alignment at south of bend is at around N17°E for section south of second bend of the left alignment.

3. Stability Assessment

To assess the stability and estimate tunnel deformation, several semi-analytical, analytical, and numerical methods were applied at various sections of the tunnel. The tunnel sections were selected with respect to overburden, rock mass type and rock mass quality. Semi-analytical approach proposed by [4] was used and analytical method consisting Convergence Confinement Method were used. Finally numerical modeling was done along the sections of both alignments.

3.1 Convergence Confinement Method (CCM)

Convergence confinement method is used to determine the relationship between Ground Reaction Curve (GRC), Longitudinal Deformation Profile (LDP), Support Characteristics Curve (SCC). The tunnel support placed after excavation does not immediately carry full pressure since a part of pressure is carried by the face itself. After passage of certain time there is increment in the pressure carried by the support provided. This method is used for optimization of support [5].

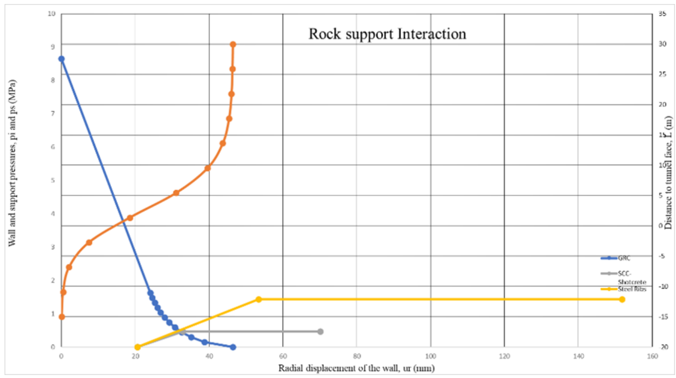

Figure 12: Schematic representation of GRC, LDP and SCC at chainage left 7+908 m

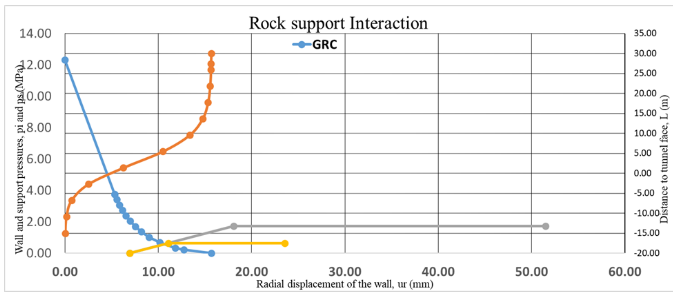

Figure 13: Schematic representation of GRC, LDP and SCC at chainage right 6+351

3.2 Panthi and Shrestha(2018) approach

Panthi and Shrestha [4] studied three different hydropower tunnels in Himalayas of Nepal for the long term squeezing phenomenon and found a relation between time-independent and time-dependent deformation using a convergence equation as proposed by [6]. It was attempted to establish a correlation between tunnel strain (both immediate and ultimate tunnel strain), vertical gravitational stress σ_v,

Table 4: Estimation of Closure by Panthi and Shrestha Approach for left alignment

Chainage	Overburden (H) m	Q-value	σ_v (Mpa)	σ_h (Mpa)	E_{rm} (Mpa)	G (Mpa)	Initial Closure ε_{ic} (%) at $P_i = 0$ MPa	Final Closure ε_{fc} (%) at $P_i = 0$ MPa	Initial Closure ε_{ic} (%) at $P_i = 1$ MPa	Final Closure ε_{fc} (%) at $P_i = 1$ MPa
1+785	68	0.56	1.89	3.01	1471.06	668.67	0.0452	0.0851	0.0103	0.0199
7+908	327	0.83	8.67	2.43	4479.35	1964.63	0.0300	0.0569	0.0069	0.0134
11+898	500	3.33	14.30	1.78	1344.91	640.43	0.6354	1.1383	0.1452	0.2674

Table 5: Estimation of Closure by Panthi and Shrestha Approach for right alignment

Chainage	Overburden (H) m	Q-value	σ_v (Mpa)	σ_h (Mpa)	E_{rm} (Mpa)	G (Mpa)	Initial Closure ε_{ic} (%) at $P_i = 0$ MPa	Final Closure ε_{fc} (%) at $P_i = 0$ MPa	Initial Closure ε_{ic} (%) at $P_i = 1$ MPa	Final Closure ε_{fc} (%) at $P_i = 1$ MPa
0+355	57	0.08	1.64	4.31	702.6091	334.57	0.668599	1.196754	0.152747	0.281094
6+351	464	5.83	12.30	2.57	8526.339	3739.62	0.022337	0.042618	0.005103	0.01001
9+694	127	33	3.53	0.96	697.5617	317.07	1.147399	2.033053	0.262132	0.477525

horizontal to vertical stress ratio k, support pressure pi, and shear modulus of rock mass (G).

3.3 Numerical Analysis

Valey model was constructed for needed cross-section of the head race tunnel in the RS2 Fem model. The bottom boundary of the model was restrained in both the directions and left-right sides of the model were restrained in both X and Y direction, the models top was free to move in both the directions. The four corners of the model were restrained to move in both the directions. Total stress can be determined using a stress cell or by considering topography, overburden, and knowledge of the overall stress conditions in the area to estimate the stress situation [7]. The input parameters Hoek and Brown constant (mi) and disturbance factor were taken from [8]. The field stress set was gravity type [9].

Table 6: Input Parameters for Right Chainage 6+351

Parameter	Value	Unit
Overburden	464	m
Poisson's Ratio	0.14	-
Tectonic Stress	3.5	MPa
Trend of Tectonic Stress	N8° E	-
Trend of Tunnel	N176° E	-
Angle between Tectonic Stress and Tunnel Length Axis	168°	-
Density of Rock Due to Gravity	0.0265	kN/m³
Vertical Stress	12.30	MPa
Horizontal Stress	2.00	MPa
Total Horizontal Stress	5.50	MPa
Horizontal Stress In-Plane	5.35	MPa
Horizontal Stress Out of Plane	2.16	MPa
Stress Ratio In Plane	0.435	-
Stress Ratio Out of Plane	0.175	-

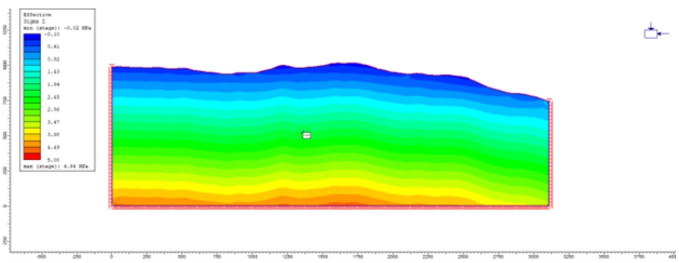

Figure 14: Valley model for headrace tunnel alignment at chainage right 6+351 m

Table 7: Input Parameters for Left Chainage 7+908

Parameter	Value	Unit
Overburden	327	m
Poisson's Ratio	0.14	-
Tectonic Stress	3.5	MPa
Trend of Tectonic Stress	N8° E	-
Trend of tunnel	N127° E	-
Angle between Tectonic Stress and Tunnel Length Axis	119°	-
Density of Rock Due to Gravity	0.0265	kN/m³
Vertical Stress	8.67	MPa
Horizontal Stress	1.41	MPa
Total Horizontal Stress	4.91	MPa
Horizontal Stress In-Plane	2.23	MPa
Horizontal Stress Out of Plane	4.09	MPa
Stress Ratio In Plane	0.257	-
Stress Ratio Out of Plane	0.472	-

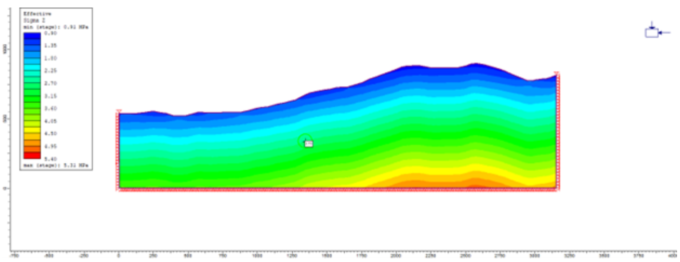

Figure 15: Valley model for headrace tunnel alignment at chainage left 7+908

3.4 Model Setup

For the analysis of the tunnel sections, a 2D box model was set up with the width of five times its excavation (5× its excavation). The in-situ stress from the valley model σ_1, σ_3, and σ_z with angle θ is used in this 2D model.The horizontal

Table 8: Output parameters for valley model

Parameters	ch.7+908	ch.6+351
σ_1 (MPa)	9.14	12.2
σ_3 (MPa)	3.71	4.95
σ_z (MPa)	2.73	2.24
θ (CCW)	117	90

stresses for the model must be projected onto the appropriate cross-section since RS2 is two-dimensional program [10].

Table 9: Input properties of support used for modeling

Shotcrete Properties	Values	Bolt Properties	Values
Shotcrete Modulus (GPa)	3	Bolt Type	Fully Bonded
Thickness (cm)	15	Length (m)	4
Poisson's ratio	0.2	Spacing (m*m)	1.5*1.5
Material Type	Plastic	Diameter (mm)	25
Peak Compressive Strength [MPa]	30	Bolt Modulus (GPa)	200
Residual Compressive Strength [MPa]	5	Tensile Capacity (MN)	0.1
Peak Tensile Strength [MPa]	5	Residual Tensile Capacity (MN)	0.01
Residual Tensile Strength [MPa]	0		
Beam Element Formulation	Timoshenko		

Elastic Analysis

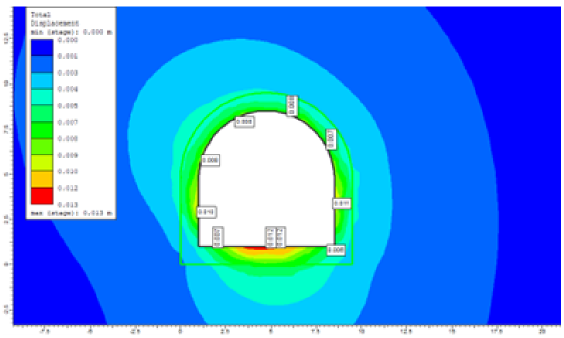

Figure 16: Strength factor before installation of support at chainage right 6+351 m

Plastic Analysis

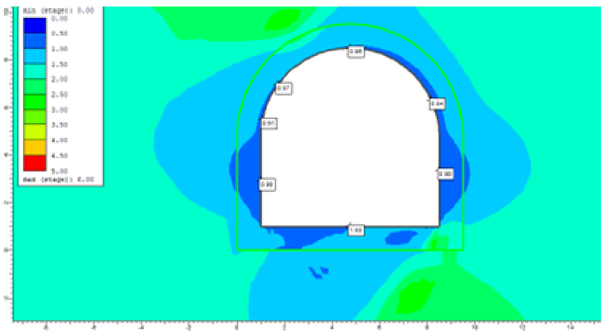

Figure 17: Total support before installation of support at chainage right 6+351 m

Plastic Analysis with Support

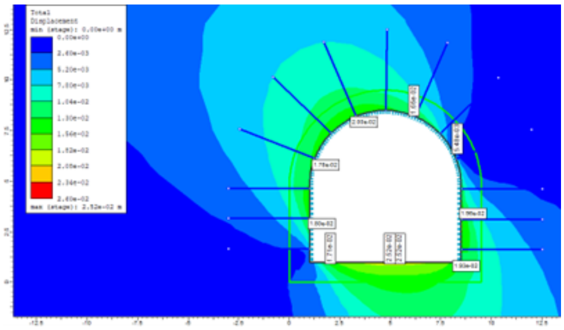

Figure 18: Total displacement after support installation at chainage right 6+351m

Elastic Analysis

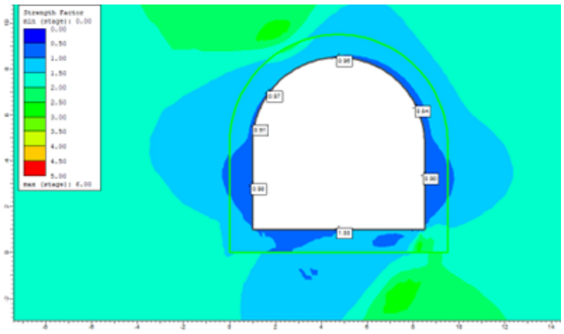

Figure 19: Strength factor before installation of support at chainage left 7+908 m

Plastic Analysis

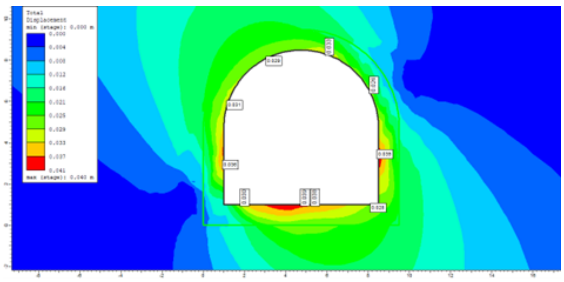

Figure 20: Total support before installation of support at chainage left 7+908m

Plastic Analysis with support

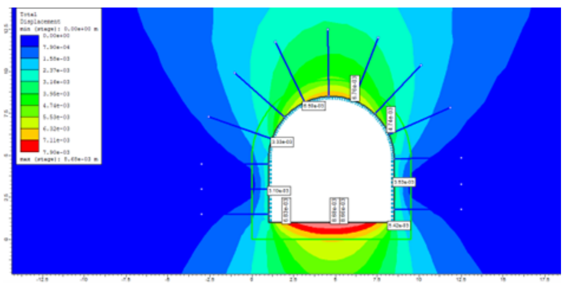

Figure 21: Total displacement after support installation at chainage left 7+908 m

4. Results and Discussions

In the project area required engineering geological and mechanical properties of rock mass were estimated on the basis of the surface mapping conducted. The discontinuity mapping output and geological map were used to select most favourable tunnel alignment. The table 4 and 5 shows the strain percentage decrease with the increase in support pressure. The initial and final closure is computed for unsupported condition and 1 MPa pressure support condition at the three sections selected at each alignment. From the semi-empirical method the maximum deformation was found at chainage 9+694m. It can be concluded that since this section had the minimum Q-value, the deformation was found to be maximum in this section. Figure 1 and 19 shows that the strength factor before installation of support is less than one in the overall periphery of the tunnel, which means that further analysis of the failure of material by plastic analysis is needed. So plastic analysis is carried out. The shows maximum displacement of tunnel (Umax) 0.039 m in left chainage 7+908 and 0.012 m in right chainage 6+351. Supports were installed at this section to obtain reduced deformation. From numerical modeling, the support to be provided at chainage 6+351m and 7+908m was found to be rock bolts and shotcrete.

5. Conclusion

In the head race tunnel, from surface mapping maximum of 65% of class 4 (poor) rock mass type was found and minimum of 1% of class 7 (exceptionally poor) rock mass type was found. Similarly, 24% class 5(very poor), 8% class 6 (extremely poor) and 2% class 3 (fair to good) rock mass type was found. The dominant rock type consisted of phyllite, with intercalation of metasandstone. To determine the necessary characteristics of the rock mass, information was gathered through geotechnical and geological mapping conducted within the study area. Semi-empirical method [4] shows the extent of deformation in different sections. The maximum initial and final closure is 1.14 mm and 2.04 mm. The numerical modeling showed that the maximum displacement of tunnel (U_{max}) at chainage $7+908$ in the left tunnel alignment is 0.039 m. Similarly the Umax at chainage $6+351$ in the right alignment is 0.012 m. Supports as mentioned in table 8 is applied. These calculated Umax values are reduced after installation of support.

Acknowledgments

The authors would like to gratefully acknowledge NORHED II Project, NTNU, Clean Energy Consultants and Department of Civil Engineering Pashchimanchal Campus for approval and providing the relevant document, site visitation, financial and moral support to conduct this research.

References

[1] Herath Gunatilake. Hydropower development and economic growth in nepal. 2020.

[2] Krishna Kanta Panthi and Bjørn Nilsen. Predicted versus actual rock mass conditions: A review of four tunnel projects in nepal himalaya. *Tunnelling and underground space technology*, 22(2):173–184, 2007.

[3] Krishna Kanta Panthi. Analysis of engineering geological uncertainties related to tunnelling in himalayan rock mass conditions. 2006.

[4] Krishna Kanta Panthi and Pawan Kumar Shrestha. Estimating tunnel strain in the weak and schistose rock mass influenced by stress anisotropy: An evaluation based on three tunnel cases from nepal. *Rock mechanics and rock engineering*, 51:1823–1838, 2018.

[5] Carlos Carranza-Torres and C Fairhurst. Application of the convergence-confinement method of tunnel design to rock masses that satisfy the hoek-brown failure criterion. *Tunnelling and underground space technology*, 15(2):187–213, 2000.

[6] J Sulem, M Panet, and A Guenot. An analytical solution for time-dependent displacements in a circular tunnel. In *International journal of rock mechanics and mining sciences & geomechanics abstracts*, volume 24, pages 155–164. Elsevier, 1987.

[7] Björn Nilsen and Arild Palmström. *Engineering Geology and Rock Engineering: Handbook*. Norwegian Group for Rock Mechanics, 2000.

[8] Evert Hoek. Analysis of rockfall hazards. *E. Hoek, Practical rock engineering*, pages 117–136, 2000.

[9] Rocscience Inc. Rocscience rs2 user guide. 2022.

[10] Bjarte Grindheim, Charlie C Li, and Are Håvard Høien. Journal of rock mechanics and geotechnical engineering. 2023.